

Generalized Reynolds number and viscosity definitions for non-Newtonian fluid flow in ducts of non-uniform cross-section

D. Crespí-Llorens^b, P. Vicente^b, A. Viedma^a

^a*Dep. Ing. Térmica y de Fluidos. Universidad Politécnica de Cartagena. Dr. Fleming, s/n (30202). Cartagena (Spain).*

^b*Dep. Ing. Mecánica y Energía. Universidad Miguel Hernández. Av. Universidad, s/n (03202). Elche (Spain). dcrespi@umh.es*

Abstract

This work presents and experimental study of the generalization method of the Reynolds number and the viscosity of pseudoplastic fluid flow in ducts of non-uniform cross-section. This method will permit to reduce 1 degree of freedom of hydrodynamical and thermal problems in those ducts. A review of the state of the art has been undertaken and the generalization equation proposed for ducts of uniform cross section has been used as a starting point. The results obtained with this equation have not been found satisfactory and a new one has been proposed.

Specifically, the procedure has been developed for two models of scraped surface heat exchanger with reciprocating scrapers. For both models, the scraper consists of a concentric rod inserted in each tube of the heat exchanger, mounting an array of plugs that fit the inner tube wall. The two models studied differ in the design of the plug.

The procedure to perform the generalization method out of experimental data is accurately detailed in the present document.

Keywords: non Newtonian, viscosity, generalized Reynolds number,
non-uniform cross-section, Power Law

1 **Nomenclature**

2	m	flow consistency index (rheological property),	[Pa.s ^{n}]
3	D	inner diameter of the heat exchanger pipe,	[m]
4	D_v	inner diameter of the viscometer pipe,	[m]
5	d	diameter of the insert device shaft,	[m]
6	D_h	hydraulic diameter $D_h = D - d$,	[m]
7	L_p	pipe length between pressure ports of test section,	[m]
8	L_v	viscometer pipe length between pressure ports ,	[m]
9	N	number of measures for each experiment	
10	P	pitch of the insert devices ,	[m]
11	p	pressure,	[Pa]
12	p_L	pressure drop by length unit,	[Pa/m]
13	Q	flow rate,	[m ³ /s]
14	S	main cross-section,	[m ²]
15	u_b	bulk velocity,	[m/s]

16 **Dimensionless numbers**

17	n	flow behaviour index (rheological property)	
18	Re	Reynolds number, $Re = \rho u_b D_h / \mu$	

- 19 f Fanning friction factor, $f = \Delta p D_h / 2 L \rho u_b^2$
- 20 ξ pressure drop constant dependent on the duct geometry
- 21 a to e correlation constants

22 Greek Symbols

- 23 α exponent of Re_b in experimental correlations, $[s^{-1}]$
- 24 γ shear rate, $[s^{-1}]$
- 25 μ fluid viscosity (exact definition indicated by the subindex), $[Pa.s]$
- 26 ϕ function of n
- 27 Ψ unknown function, $[kg/m^3]$
- 28 ρ fluid density, $[kg/m^3]$
- 29 τ shear stress, $[Pa]$

30 Subscripts

- 31 b Reynolds number or viscosity defined by Eq. 2
- 32 g Reynolds number or viscosity defined by Eqs. 18 and 19
- 33 MR defined by Metzner and Reed (1955) (Eqs. 4 and 5)
- 34 DL defined using the equation from Delplace and Leuliet (1995) (Eqs.
35 6 and 7)
- 36 $\xi = an$ generalization based on pressure drop in annulus, where ξ is ob-
37 tained from Kozicki et al. (1966))

38 $\xi = exp \xi$ in Eqs. 6 and 7 is obtained by experimental correlation

39 v belonging to the viscometer

40 w at the inside pipe wall

41 1. Introduction

42 Many fluids in the food and chemical or petrochemical industries are
43 non-Newtonian. In such applications the determination of parameters such
44 as the friction factor and the Nusselt number is necessary for the calculation
45 of pressure losses and heat transfer rates or temperature distributions in heat
46 exchangers. This can be achieved experimentally or theoretically by solving
47 the appropriate transport equations for typical common geometries (circular
48 ducts, flat ducts, etc.). An important characteristic of these fluids is that
49 they have large apparent viscosities; therefore, laminar flow conditions occur
50 more often than with Newtonian fluids.

51 Pseudoplastic fluids are the most common non-Newtonian fluids in the
52 process industry Chhabra and Richardson (2008); Cancela et al. (2005). For
53 this fluids, in a certain range of shear stress, the viscosity decreases as shear
54 stress increases. To describe this behaviour, various mathematical models
55 can be used. Among them, the Power Law model is widely used because of
56 its simplicity. The model can be used to explain the viscosity of a specific
57 fluid in a limited range of shear rates. The Power Law model (Eq. 1) has two
58 parameters: the flow behaviour index n and the flow consistency index m .
59 Thus, the hydrodynamic and thermal problems have one additional degree

60 of freedom, which increases their complexity.

$$\tau = m\gamma^n \quad (1)$$

61 For example, let us consider the study of pressure drop in fully developed
 62 flow in pipes for forced convection. The list of significant variables can be
 63 $p_L = \Psi(D, u_b, \rho, m, n)$. Through the Pi Theorem the problem simplifies to
 64 three non-dimensional numbers $f = \Psi(Re, n)$. Consequently, the relation
 65 between Re and the friction factor will be different for fluids with different
 66 n . With the previous list of variables, the Reynolds number for power law
 67 fluids would be,

$$Re_b = \frac{\rho u_b^{2-n} D^n}{m} = \frac{\rho u_b D}{\mu_b} \quad (2)$$

68 , where viscosity would be defined by $\mu_b = m(u_b/D)^{n-1}$. Other viscosity
 69 definitions, with the same dimensional equations, are possible and will be
 70 more useful for the study of pressure drop in heat exchangers.

71 Metzner and Reed (1955) were the first to use the so called generalization
 72 method. They analytically obtained the relation between the friction factor
 73 f and the Reynolds number Re_b for the fully developed laminar flow in a
 74 pipe. Then, they defined a new Reynolds number Re_{MR} , being the one
 75 which multiplied by the friction factor gave the same result that the one
 76 given by a Newtonian fluid.

$$f \times Re_{MR} = 16 \quad (3)$$

$$Re_{MR} = \frac{\rho u_b^{2-n} D^n}{m 8^{n-1} ((3n+1)/(4n))^n} = \frac{\rho u_b D}{\mu_{MR}} \quad (4)$$

78 , being the generalized viscosity for the flow in pipes

$$\mu_{MR} = m \left(\frac{u_b}{D_h} \right)^{n-1} 8^{n-1} \left(\frac{3n+1}{4n} \right)^n \quad (5)$$

79 Kozicki et al. (1966) obtained a relation between friction factor and Reynolds
80 number for various simple geometries (circular pipes, parallel plates, concen-
81 tric annuli and rectangular, isosceles triangular and elliptical ducts) as a
82 function of two parameters. Afterwards, Delplace and Leuliet (1995) re-
83 duced those parameters to one. Therefore, the definition of Metzner and
84 Reed (1955) can be applied to geometries with uniform cross-section as a
85 function of a single geometric constant.

$$Re_{DL} = \frac{\rho u_b^{2-n} D_h^n}{m \times \xi^{n-1} \left(\frac{24n+\xi}{(24+\xi)n} \right)^n} \quad (6)$$

$$\mu_{DL} = m \left(\frac{u_b}{D_h} \right)^{n-1} \xi^{n-1} \left(\frac{24n+\xi}{(24+\xi)n} \right)^n \quad (7)$$

$$f \times Re_{DL} = 2\xi \quad (8)$$

88 For duct geometries of uniform cross-section different from the ones stud-
89 ied by Kozicki et al. (1966), similar relations can be obtained either exper-
90 imentally or numerically. This simplification leads to significant reduction
91 in the study cases of a particular problem. This has been called a general-
92 ization method because it allows to express the pressure drop behaviour of
93 Newtonian and non-Newtonian fluids with a single curve. Consequently, the
94 Reynolds number and viscosity defined by this method are known as the *gen-
95 eralized Reynolds number* and the *generalized viscosity* (Kakaç et al., 1987;
96 Chhabra and Richardson, 2008). Besides, the generalized viscosity can be
97 used to generalize other dimensionless numbers such as the Prandtl number
98 in non isothermal flows (Hartnett and Kostic, 1985; Delplace and Leuliet,
99 1995).

100 The described method has been used by many authors until recent days
101 (Gratao et al., 2006, 2007; Giri and Majumder, 2014). But, as mentioned

102 before, it can only be applied to ducts with uniform cross-section, where the
103 shear-stress at the wall is uniform along the duct.

104 Enhanced heat exchangers EHE (Hong and Bergles, 1976; Marner and
105 Bergles, 1985) are widely used in the process industry in order to enhance
106 heat transfer and they work often with non-Newtonian fluids. Webb (2005)
107 classified enhancement techniques into active, if they require external power,
108 and passive, if they do not. Active techniques as scraped surface heat ex-
109 changers SSHE are specially designed to avoid fouling and enhance heat
110 transfer. This last kind of enhanced heat exchanger is specially useful for the
111 work with non-Newtonian fluids because of their high viscosity (Nazmeev,
112 1979). In most EHE designs, specially in SSHE, the cross-section varies along
113 their length or else the cross-section is uniform but complex and has not pre-
114 viously been studied. Therefore, the generalization method must be based
115 on experimental or numerical results and it is not straightforward.

116 To overcome this inconvenience, most authors have considered their geom-
117 etry to be very similar to one of the simple uniform cross-section geometries
118 studied by Kozicki et al. (1966) or Metzner and Reed (1955). This is the case
119 of corrugated pipes or pipes with wire coil or twisted tape inserts. Manglik
120 et al. (1988); Oliver and Shoji (1992); Patil (2000); Martínez et al. (2014)
121 took this option for their studies of passive EHE performance with non-
122 Newtonian fluids and Igumentsev and Nazmeev (1978) did so for his study
123 of SSHE. However, there are complex geometries where this assumption is
124 not valid at all. For those cases, Delplace and Leuliet (1995) proposed the
125 use of experimental methods to obtain the value of ξ . Based on the previous
126 research of Rene et al. (1991), they proposed to use $\xi = 56.6$ for a plate heat

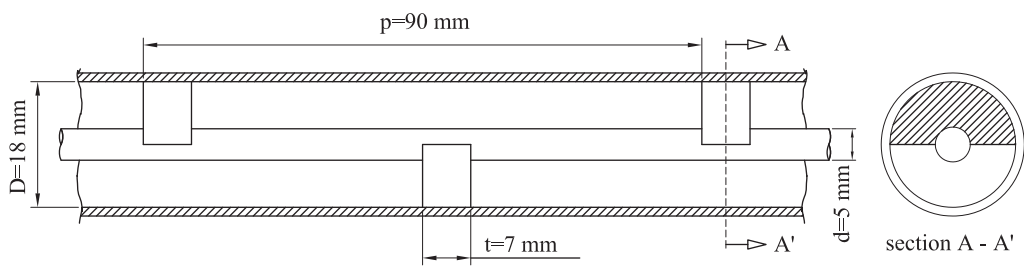
127 exchanger type. Afterwards some other researchers have broaden Rene et al.
128 (1991) and Delplace and Leuliet (1995) studies with numerical simulations in
129 the same plate heat exchangers model (Fernandes et al., 2007, 2008) varying
130 some design parameters.

131 Our extensive literature search has not yielded further researches about
132 the generalization method of viscosity in complex geometries with non-uniform
133 cross section. In view of this situation the present study was undertaken.

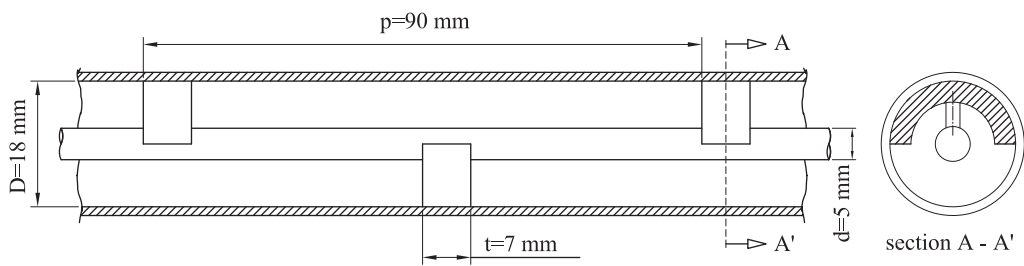
134 The present paper presents a simplified generalization method for the
135 Reynolds number and fluid viscosity, based on the studies of Metzner and
136 Reed (1955) and Delplace and Leuliet (1995), which can be applied to ducts
137 of non-uniform cross-section. In order to prove its validity, pressure drop
138 has been measured experimentally in two different pipe axial reciprocating
139 scraped surface heat exchangers AR-SSHE. These geometries are shown in
140 Fig. 1.

141 **2. Experimental Set-up**

142 The experimental setup shown in Fig. 2 has been used to measure pressure
143 drop for different flow regimes in axial reciprocating scraped surface heat
144 exchangers (Fig. 1(a) and Fig. 1(b)). The experimental facility consists of
145 two independent circuits. The primary circuit, which contains the test fluid,
146 is divided in two sub-loops. The test section is placed in the main one,
147 including a gear pump (2) driven by a frequency controller (3). The test
148 fluid in the supply tank (1) is continuously cooled in the second sub-loop
149 through a plate heat exchanger (13) with a coolant flow rate settled by a
150 three-way valve (15). The coolant liquid of the secondary circuit is stored in



(a) EG1 geometry of an scraped surface heat exchanger.



(b) EG2 geometry of an scraped surface heat exchanger.

Figure 1: Analysed geometries.

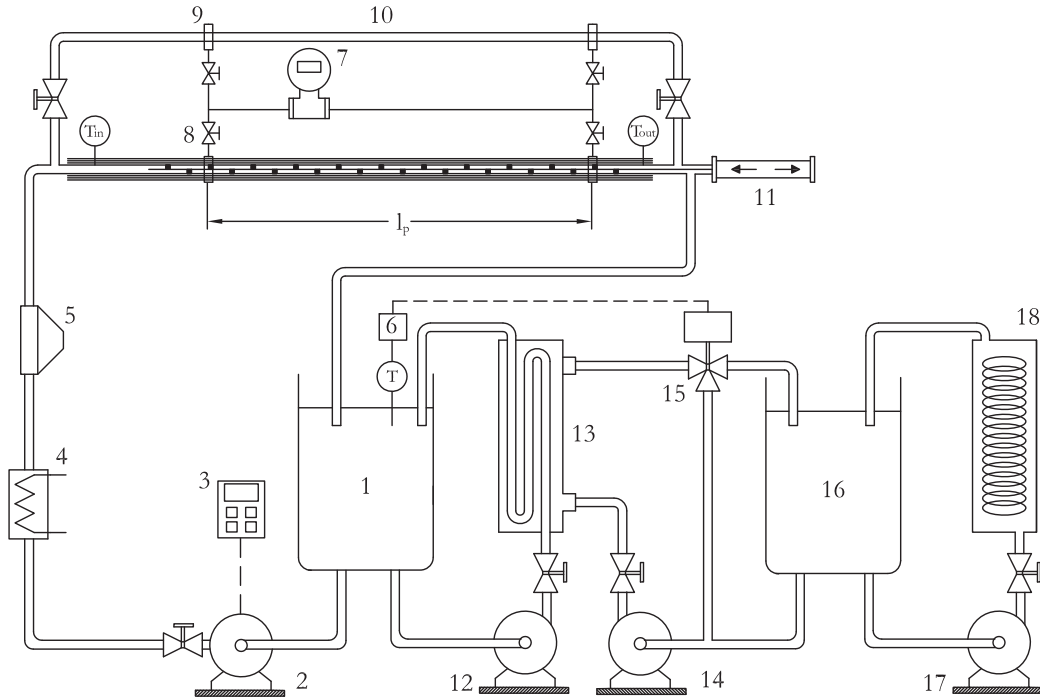


Figure 2: Experimental set-up. (1) Test fluid tank, (2, 12) gear pumps, (3) frequency converter, (4) immersion resistance, (5) Coriolis flowmeter, (6) temperature sensor and PID controller. (7) pressure transmitter, (8) stainless steel tube with an insert scraper, (9) pressure ports, (10) smooth stainless steel pipe used as viscometer, inlet and outlet immersion RTDs, (11) hydraulic piston (14, 17) centrifugal pumps, (15) three-way valve, (16) coolant liquid tank, (18) cooling machine.

151 a 1000 l tank (16) from where it flows to a cooling machine. The thermal
152 inertia of this tank, with a capacity of 1000 l, together with the operation of
153 the PID-controlled three way valve provides stability to the temperature of
154 the test fluid in the supply tank, which can be accurately fixed to a desired
155 value. The test section was placed in the main circuit and consisted of a
156 thin-walled, 4 m long, 316L stainless steel tube with an insert scraper. The
157 inner and outer diameters of the tube were 18 mm and 20 mm, respectively.
158 Two oversize, low-velocity gear pumps (one on each circuit) were used for
159 circulating the working fluid, in order to minimize fluid degradation during
160 the tests. Mass flow rate and fluid density was measured by a Coriolis flow
161 meter, which performs properly when working with non-Newtonian fluids
162 (Fyrippi et al., 2004). Four pressure taps separated by 90° were coupled to
163 each end of the pressure test section of 1.85 m length. A long test section has
164 been used to improve measurement precision. Pressure drop Δp_{E1} and Δp_{E2}
165 was measured by means of two highly accurate pressure transmitters LD-301
166 configured for different ranges. Pressure measurement ports were separated a
167 distance $L_p = 20 \times P$, and consisted of four pressure holes peripherally spaced
168 by 90° . Test section was preceded by a development region of $L_e = 6 \times P$
169 length, in order to establish periodic flow conditions.

170 The rheological properties of the non-Newtonian test fluid n and m is
171 measured by an in-line viscometer, parallel to the testing tube. In that way,
172 measurements of the rheological properties could be done at the beginning
173 and at the end of each set of experiments, minimizing the thixotropy effect.
174 Further details are given in next section.

175 Further details of the working apparatus and the calibration procedure

176 are given in Solano et al. (2011) and García et al. (2005).

177 *2.1. Test fluid characteristics*

178 The test fluid was 1% wt aqueous solutions of carboxymethyl cellulose
179 (CMC), supplied by SigmaAldrich Co. CMC with different chain length
180 have been used: medium viscosity (ref. C4888, 250 kDa), high viscosity (ref.
181 C5013, 700 kDa) and ultra high viscosity (ref. 21904). The solutions were
182 prepared by dissolving the polymer powder in distilled water and then raising
183 the pH values of the solution to increase viscosity. This fluid shows a non-
184 Newtonian pseudoplastic behaviour well described by the Power Law model
185 of Eq. 1 for a big range of shear rates (Abdelrahim and Ramaswamy, 1995;
186 Ghannam and Esmail, 1996; Abu-Jdayil, 2003; Yang and Zhu, 2007), al-
187 though it presents a Newtonian plateau for shear rates under 0.1 s^{-1} (Bench-
188 abane and Bekkour, 2008).

189 All CMC thermophysical properties but the rheological parameters and
190 fluid density were assumed to be the same as pure water (Chhabra and
191 Richardson, 2008; Cancela et al., 2005).

192 Rheological fluid properties are strongly influenced by the type of CMC
193 powder employed, the preparation method and fluid degradation due to shear
194 stress and thermal treatment. The combination of those factors allows to
195 obtain fluids with different pseudoplastic behaviour, ranging from $n = 0.45$
196 to $n = 1$.

197 The values of n and m for the test fluid were obtained by using the in-line
198 smooth pipe as a viscometer. In the smooth pipe, flow rate Q and pressure
199 drop Δp are measured 20 times for four different flow rates. Bulk velocity
200 u_b and shear stress at the wall τ_w are obtained out of flow rate and pressure

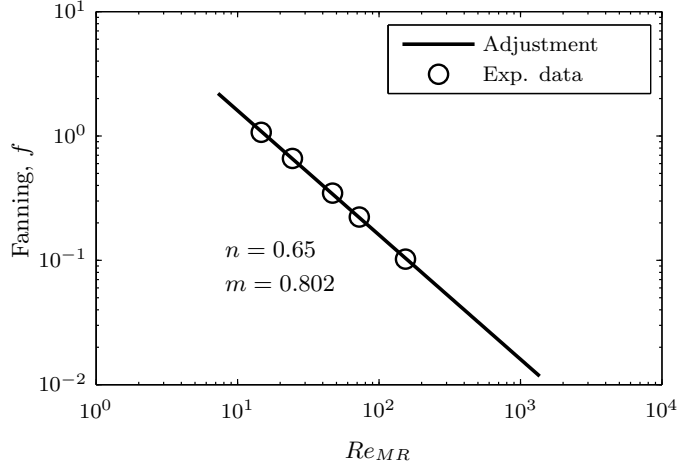


Figure 3: Rheological properties measurement during one of the test.

201 drop respectively

$$\tau_w = \frac{\Delta p D_v}{4L} \quad (9)$$

202 , as the velocity profile of the fully developed isothermal flow of power law
 203 fluids in pipes is well known, τ_w can also be derived from the constitutive
 204 Eq. 1,

$$\tau_w = m \left[\frac{8u_b}{D_v} \left(\frac{3n+1}{4n} \right) \right]^n \quad (10)$$

205 , whose logarithm yields

$$\ln(\tau_w) = n \times \ln(u_b) + \ln(m) + n \times \ln \left[\frac{8u_b}{D_v} \left(\frac{3n+1}{4n} \right) \right] \quad (11)$$

206 , out of which the rheological properties m and n can be obtained by ad-
 207 justing the experimental data with a least squared method. An example of
 208 a rheological measurement result is shown in Fig. 3.

209 Because of fluid degradation, rheological properties must be obtained fre-
210 quently. Experiments are planned in sets of 15 to 25 and rheological proper-
211 ties are obtained before and after each set. A maximum of 3% deviation be-
212 tween rheological properties measurements has been obtained. Degradation
213 between measurements has been supposed to be linear with experimenting
214 time, so that m and n can be obtained for each experiment.

215 *2.2. Accuracy of the experimental data*

216 The experimental uncertainty was calculated by following the "Guide to
217 the expression of uncertainty in measurement", published by the ISO (1995).
218 On one hand, the Coriolis flowmeter has a repeatability of 0.025 % of the
219 flow rate measure, while its precision when measuring density is 0.2 kg/m³.
220 On the other hand, pressure sensor has a repeatability of 0.075 of its range.
221 Uncertainties of the heat exchanger and viscometer dimensions have been as-
222 signed according to the measuring tool employed. The uncertainty associated
223 to rheological properties are obtained out of the least squares adjustment.
224 The maximum uncertainty of n and m are 0.01% and 0.4% respectively.

225 A summary of the uncertainties of dimensions and sensor measurements
226 is shown in Table 1. The resulting error for Re_b and f are of 1.2% and 2%
227 respectively.

228 **3. Results**

229 Friction factor measurements in EG1 and EG2 geometries are plotted in
230 Fig 4 versus Re_b defined by Eq. 2. As it can be appreciated the friction factor
231 f is a function of Re_b and the flow behaviour index n .

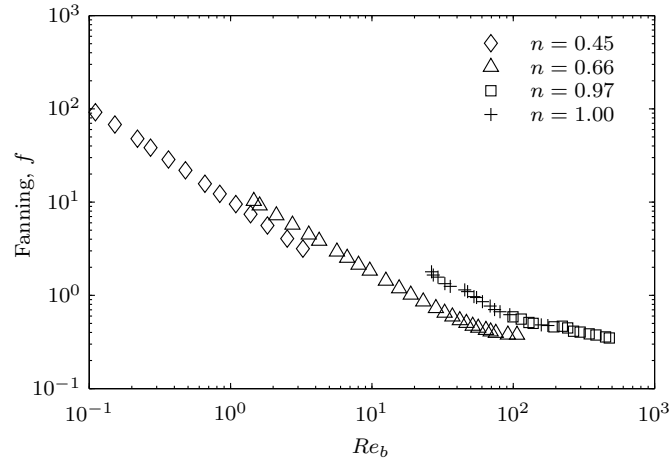
(a) Dimensions.

Variable	Value	Uncertainty	Units	Uncert. (%)
D	18	$0.05/\sqrt{3}$	mm	0.2
d	5	$0.05/\sqrt{3}$	mm	0.6
D_h	13	0.04	mm	0.3
S	234.8	0.7	mm ²	0.4
D_v	16	$0.05/\sqrt{3}$	mm	0.2
S_v	201.1	0.8	mm ²	0.4
L_v	1885	$0.5/\sqrt{3}$	mm	0.02
L_p	1850	$0.5/\sqrt{3}$	mm	0.02

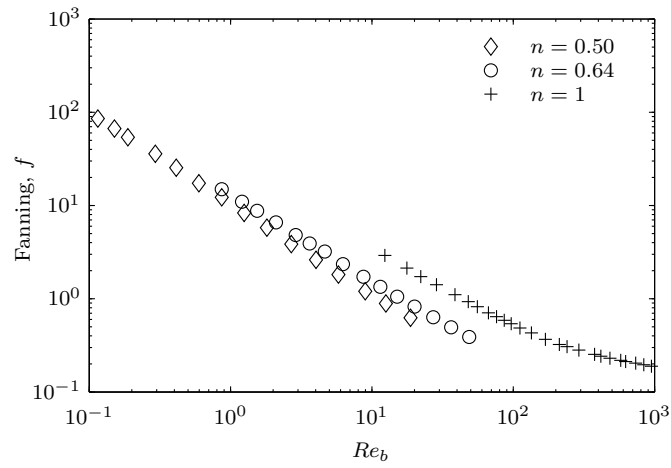
(b) Sensors measurements. N is the number of measurements.

Variable	Value	N	Uncertainty	Units	Max. Uncert. (%)
Δp_{E1}	10 – 405	20 – 10	0.07 – 0.09	mbar	0.7
Δp_{E2}	400 – 2500	10	0.6	mbar	0.1
Q	30 – 2000	10 – 20	-	kg/h	7.9×10^{-3}
ρ	1000	1	0.1	kg/m ³	0.01

Table 1: Uncertainties in dimensions and sensor measurements.



(a) EG1



(b) EG2

Figure 4: Re_b versus Fanning friction factor for the geometries under study. Only most representative results are shown.

232 *3.1. Generalization based on annulus geometry*

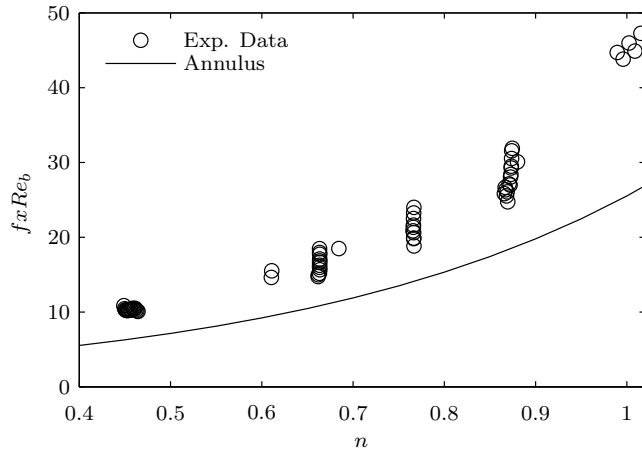
233 Geometries of EG1 and EG2 scraped surface heat exchangers are similar
234 to an annular passage. Therefore, a generalization method based on the
235 annulus geometry may be a good approach for these cases. For this value of
236 the radius ratio ($d/D = 5/18$), the value of $\xi = 11.69$ can be obtained from
237 Kozicki et al. (1966).

238 In Fig. 5, $f \times Re_b$ versus n has been plotted for the experiments and for
239 the solution in annulus given by Eq. 6 with $\xi = 11.69$. As it can be observed,
240 annulus results underpredict experimental ones in 34% on average for EG1
241 and in 27% on average for EG2. Pressure drop results are shown in Fig. 6
242 and Fig. 7, where the generalized Reynolds number has been defined for
243 the mentioned value of ξ . As it can be observed, the results show different
244 curves for each fluid with different value of n and measurements do differ
245 from the theoretical solution in annulus. Therefore it can be concluded that
246 the generalization method is not valid in these cases.

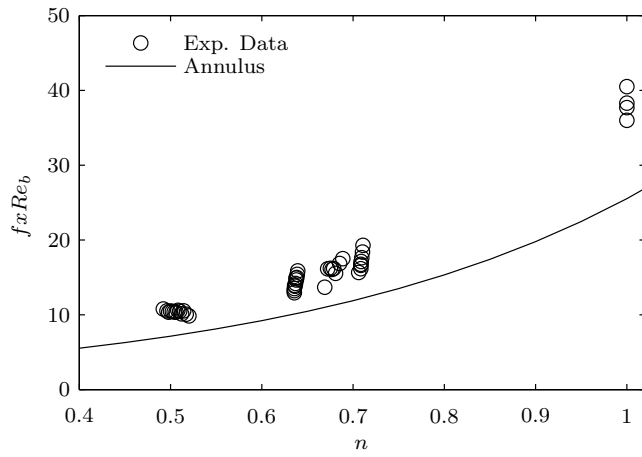
247 However, some useful information can be obtained from Figures 6 and
248 7. For $Re_{DL,\xi=an} < 100$ the flow is laminar and above this range the tran-
249 sitional flow starts. Besides, it can be observed that the distance between
250 experimental results and the line representing the annulus solution varies
251 with $Re_{DL,\xi=an}$, meaning that $f \not\propto Re_b^{-1}$.

252 *3.2. Experimental value of ξ*

253 In this subsection, the solution suggested by Delplace and Leuliet (1995)
254 has been used for the generalization method. They proposed to use Eq. 8,
255 what has been modified to include an exponent for the Reynolds number, α ,

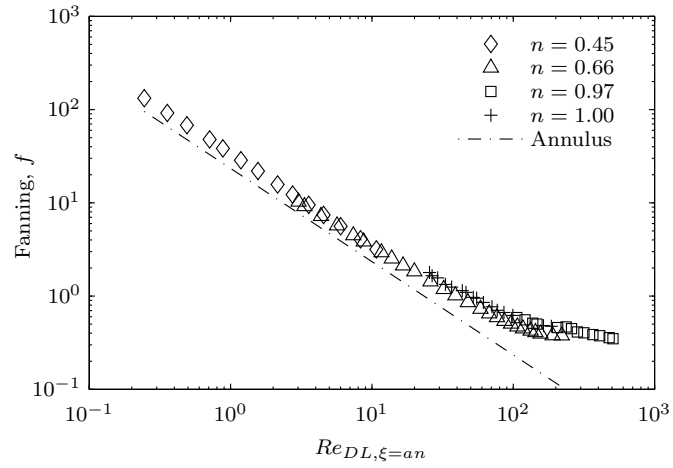


(a) EG1

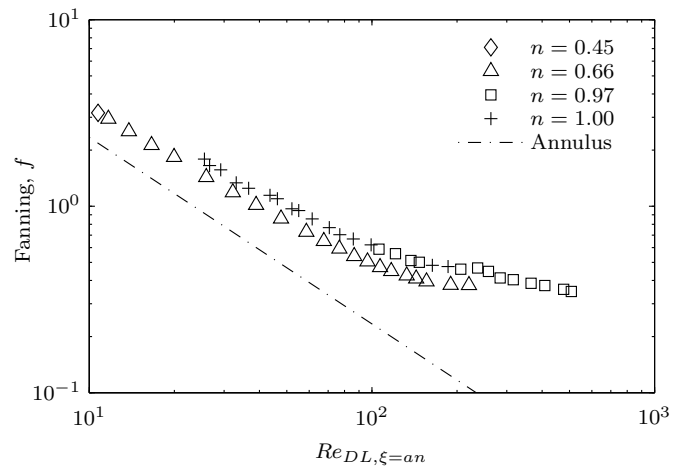


(b) EG2

Figure 5: Comparison of $f \times Re_b$ between experimental results and theoretical results for annulus.

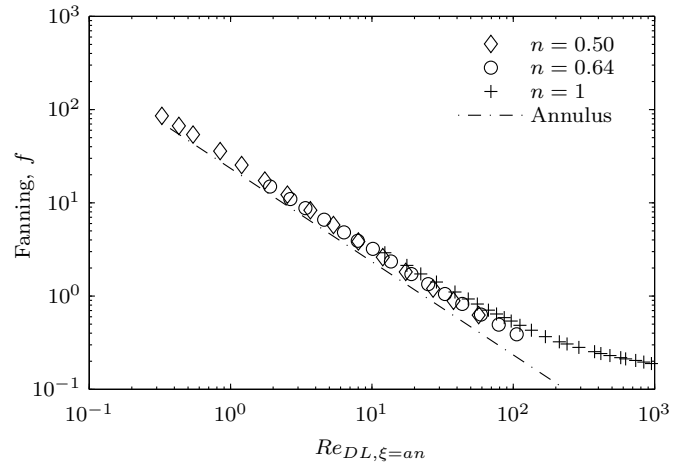


(a) Whole Reynolds range

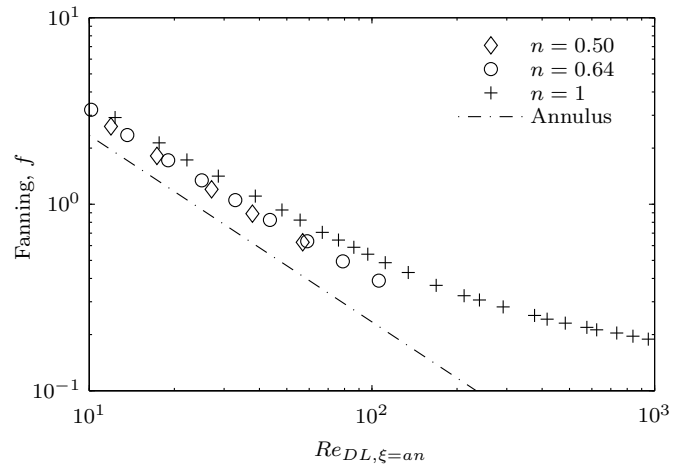


(b) Narrower Reynolds range

Figure 6: EG1. $Re_{DL, \xi=an}$ versus Fanning friction factor.



(a) Whole Reynolds range



(b) Narrower Reynolds range

Figure 7: EG2. $Re_{DL, \xi=an}$ versus Fanning friction factor.

256 as it has been explained in previous section,

$$f \times Re_b^\alpha = 2\xi^n \left(\frac{24n + \xi}{(24 + \xi)n} \right)^n \quad (12)$$

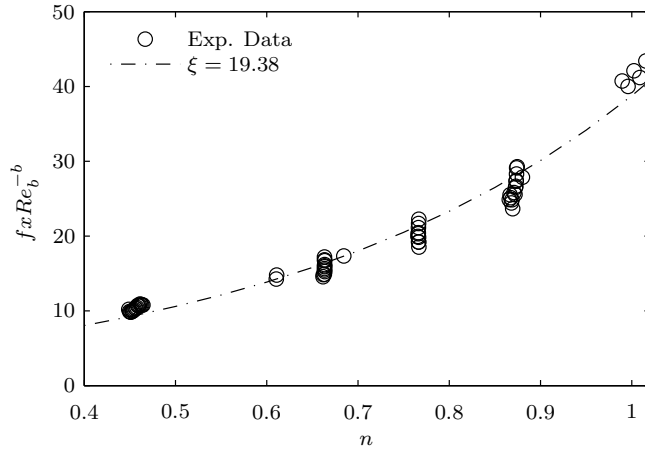
257 The experimental data has been correlated to obtain the value of ξ in
 258 Eq. 12. For this, only experiments with Reynolds numbers under 40 (highly
 259 laminar region) have been considered. The reason for doing this is that,
 260 although laminar region ends at Reynolds number about 100, the exponent
 261 of the Reynolds number in Eq. 12 decreases with the Reynolds number along
 262 the laminar region, what becomes significant for Reynolds numbers above
 263 40. The goal is not to obtain an experimental correlation for the data in the
 264 laminar region but to obtain a proper definition of the generalized Reynolds
 265 number, valid for the whole laminar region.

266 The experimental values of ξ for EG1 and EG2, and the corresponding
 267 uncertainties for a confidence level of 95 % are shown in Table 2¹. The exper-
 268 imental data and Eq. 12 with the calculated values of ξ for both geometries
 269 are plotted in Fig. 8. Besides, friction factor versus the generalized Reynolds
 270 number (with this ξ) is plotted in Fig. 9.

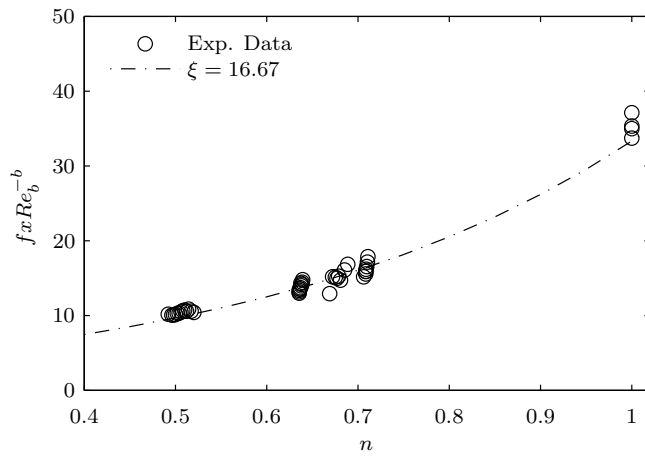
Table 2: Experimental correlation for ξ in Eq. 12 (Delplace and Leuliet, 1995).

	α	ξ	Error
EG1	0.974	19.38	17.0%
EG2	0.951	16.67	13.3%

¹The procedure to obtain α is explained in section 3.4.

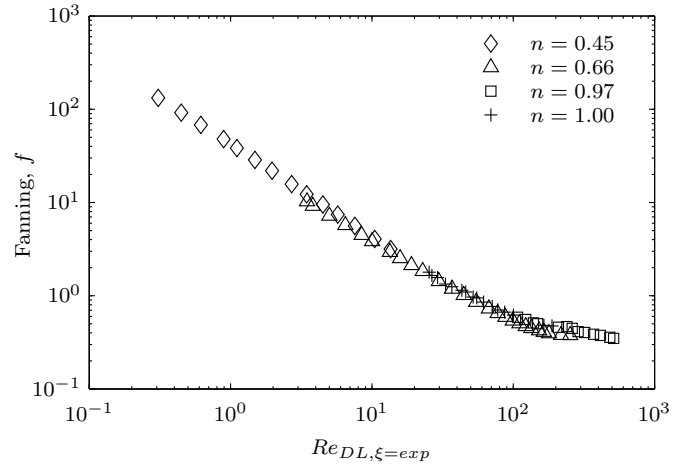


(a) EG1

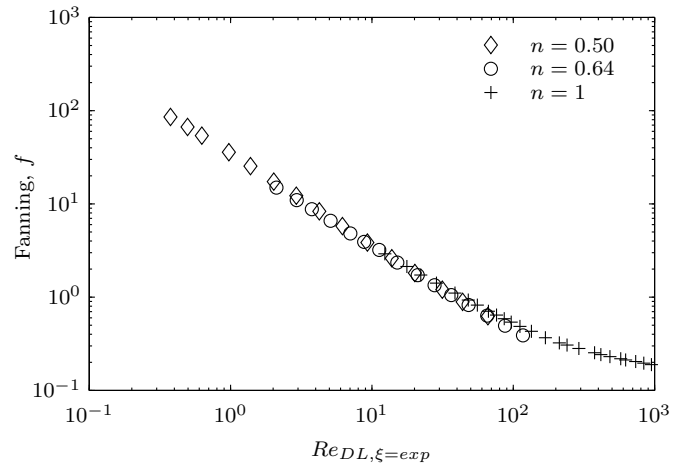


(b) EG2

Figure 8: Comparison between experimental results and Eq. 12 with the experimental values of ξ (see Table 2)



(a) EG1



(b) EG2

Figure 9: Generalized Reynolds number with Eq. 12 and the experimental values of ξ (see Table 2).

271 Results in Fig. 8 show an under prediction of the product $f \times Re_b^\alpha$ for
 272 $n \approx 0.45$ and $n \approx 1$ for both geometries. Furthermore, it can be observed in
 273 Fig. 9 that the experimental results for different n do not collapse to the same
 274 curve. This effect is higher in EG1 geometry, where the flow is significantly
 275 different from the annulus geometry. Results of this generalization method
 276 are still not satisfactory.

277 3.3. Proposed experimental correlations

278 At this point, an experimental correlation for $f \times Re_b^\alpha$ must be obtained
 279 in order to apply the generalization method properly. With this objective,
 280 different expressions will be tested:

- 281 1. Expression with two parameters,

$$f \times Re_b^\alpha = a c^{n-1} \quad (13)$$

- 282 2. Expression with three parameters,

$$f \times Re_b^\alpha = a c^{n-1} n^d \quad (14)$$

- 283 3. Expression with four parameters,

$$f \times Re_b^\alpha = a \left(\frac{c n^2 + d n + e}{(c + d + e)n^2} \right)^n \quad (15)$$

284 , where a , c , d and e are correlation constants (the letter b has been omitted
 285 to avoid confusion). As in previous section, the exponent of the Reynolds
 286 number α has been included due to the peculiar nature of the AR-SSHE,
 287 where the flow does not exactly behave as in a uniform cross section geometry.

Table 3: Correlation results.

(a) EG1.			
	Ec. 13	Ec. 14	Ec. 15
α	0.974	0.974	0.974
a	39.742	41.403	41.729
c	15.536	262.27	212.8
d		-2.1177	-319.16
e			158.93
Error (%)	15.9	11.4	9.6
(b) EG2.			
	Ec. 13	Ec. 14	Ec. 15
α	0.951	0.951	0.951
a	33.786	34.070	34.078
c	12.574	80.555	75.852
d		-1.4419	-95.224
e			50.102
Error (%)	12.7	9.0	9.0

288 The results of the different approaches can be seen in Table 3¹. The three
 289 correlations proposed perform better than the one proposed by Delplace and
 290 Leuliet (1995). The lower error corresponds to Eq. 15 followed by Eq. 14,
 291 both presenting good agreement with experimental data. Both correlations
 292 are plotted in Fig. 10 versus experimental results.

293 To our understanding, Eq. 14 offers a good approach to experimental
 294 results with just three parameters, two of which will appear in the generalized
 295 viscosity definition.

296 In order to define a generalized Reynolds number and viscosity, according
 297 to Delplace and Leuliet (1995) $\phi(1) = 1$ in Eq. 16, so

$$Re_g = \frac{Re_b}{\phi(n)} \quad (16)$$

298 , consequently

$$\phi(n) = c^{n-1} n^d \quad (17)$$

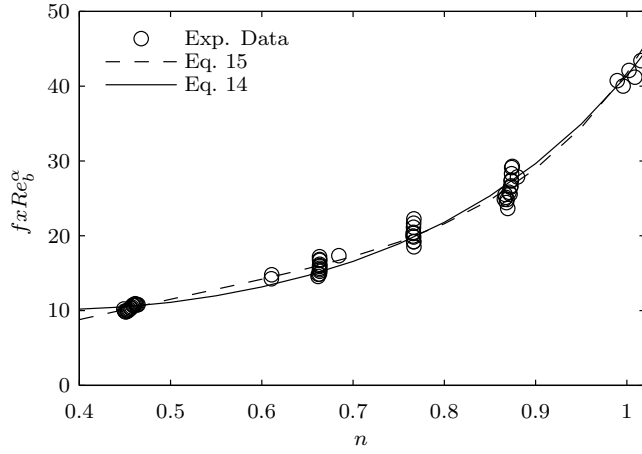
$$Re_g = \frac{\rho u_b^{2-n} D^n}{m c^{n-1} n^d} \quad (18)$$

$$\mu_g = m c^{n-1} n^d \left(\frac{u_b}{D_h} \right)^{n-1} \quad (19)$$

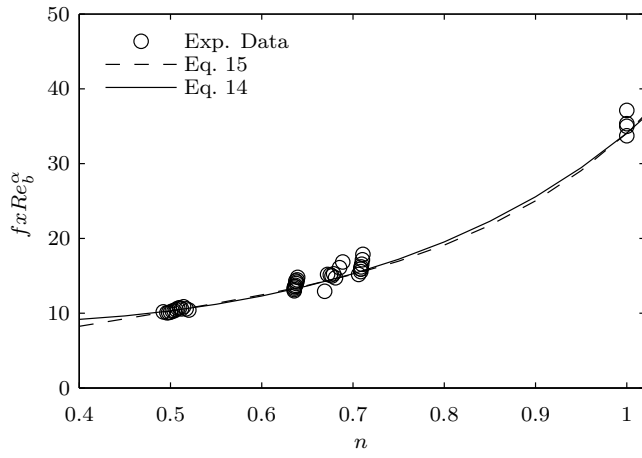
301 Pressure drop results are shown in Fig. 11 and Fig. 12 with the generalized
 302 Reynolds number defined by Eq. 18. The figure shows as the experimental
 303 data for fluids with different pseudoplastic behaviour (different n) can be rep-
 304 resented with a single curve in the laminar flow region, while some differences
 305 arise in transition flow region.

306 The proposed generalization method has more parameters than the equa-
 307 tion from Delplace and Leuliet (1995), but correlates better with the ex-

¹The procedure to obtain α is explained in section 3.4.



(a) EG1



(b) EG2

Figure 10: Comparison between experimental results and experimental correlations.

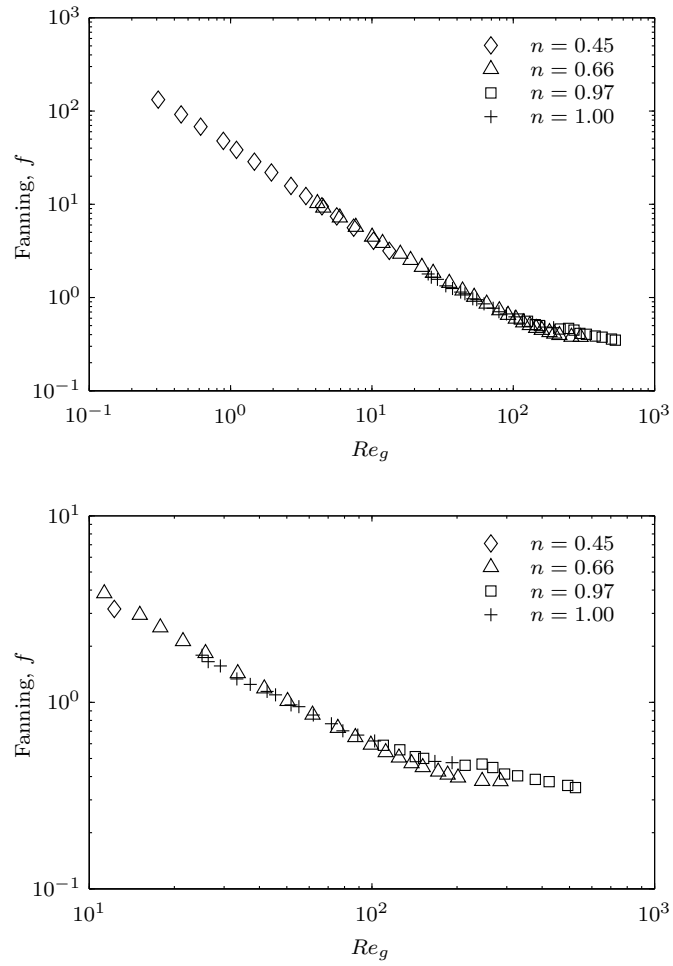


Figure 11: EG1. Generalized Reynolds number Re_g (Eq. 18) versus Fanning friction factor.

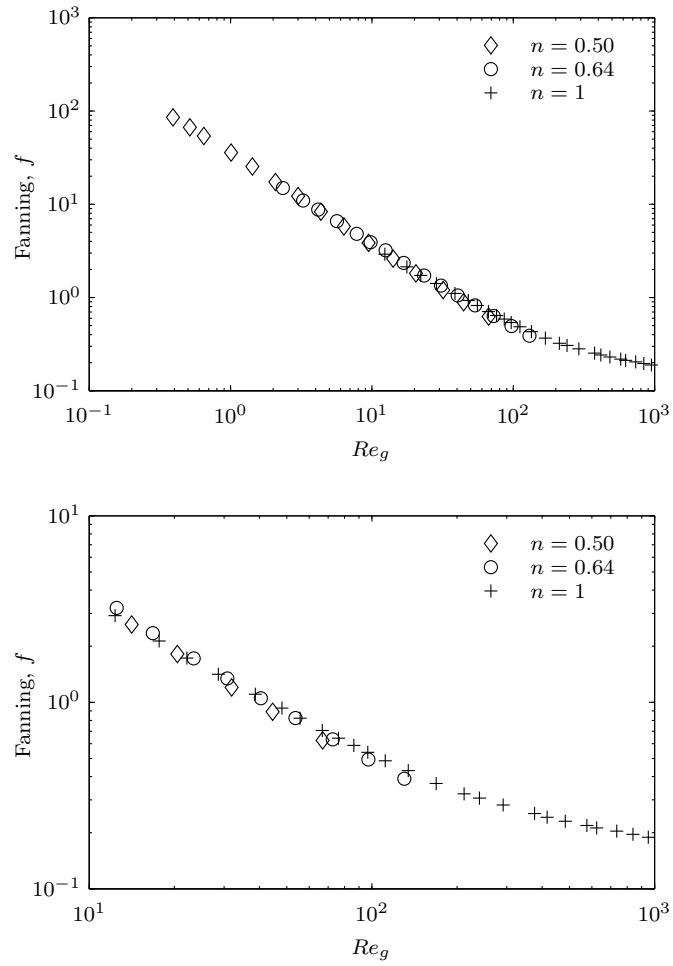


Figure 12: EG2. Generalized Reynolds number Re_g (Eq. 18) versus Fanning friction factor.

308 perimental data, being still very simple (see Table 2 and Table 3). This
309 generalization method allows to reduce complexity in hydrodynamical prob-
310 lems, where the dependence of n is included in the viscosity definition. The
311 method can be followed in similar heat exchangers devices in order to obtain
312 a valid expression for the generalized viscosity and the generalized Reynolds
313 number.

314 The expression obtained for the generalized Reynolds number and vis-
315 cosity (Eq. 18 and Eq. 19) will be valid for this design of heat exchanger,
316 working with any non Newtonian fluid whose behaviour can be modelled
317 with the Power Law model. Obviously, care must be taken that the values
318 of m and n , obtained for the working fluid, are valid in the working range of
319 shear stress.

320 *3.4. Additional comments on the experiments and the correlations obtained*

321 A total of 161 experiments for the EG1 geometry and 101 for EG2 have
322 been carried out. Those experiments belong to laminar, transition and tur-
323 bulent regions. For all the correlations in this work, only experiments under
324 $Re_g < 40$ have been used to ensure they belong to the laminar region. All
325 the experiments with $Re_g < 40$ are represented in Figures 5, 8 and 10. As,
326 at first, the definition of Re_g is unknown, the first selection has been done by
327 using $Re_{DL,\xi=an} < 40$ and corrected with Re_g at the end if necessary. The
328 number of experiments which satisfy the previous condition are 61 and 47
329 for EG1 and EG2 geometries respectively. In spite of the restriction imposed
330 ($Re_g < 40$), in Figures 11 and 12 it can be appreciated that the behaviour
331 of the different fluids in the AR-SSHE is represented by a single curve in the
332 whole laminar region ($Re_g < 100$). This means that the generalized Reynolds

333 number and viscosity definitions are valid in that range.

334 In order to perform correlations of equations 12, 13, 14 and 15, the expo-
335 nent of the Reynolds number α has been obtained first. For that, a correlation
336 for the friction factor has been obtained in $f = \Psi(Re_b, n)$ as indicated by
337 each equation. Afterwards, that value of the exponent α has been used to
338 correlate $f \times Re_b^\alpha$ as a function of n according to each equation. This proce-
339 dure allows to minimize the correlating error due to high scaling differences
340 in the Fanning friction factor.

341 4. Conclusions

342 In this work, a generalization method in ducts of non uniform cross-
343 section has been presented and experimentally evaluated in two commercial
344 scraped surface heat exchangers.

- 345 • Pressure drop of a pseudoplastic non-Newtonian fluid has been ex-
346 perimentally determined in two scraped surface heat exchangers (EG1
347 and EG2) in static conditions. Experiments have been carried out in
348 a wide range of Reynolds numbers $Re_g = [0.3, 600]$ and with Newto-
349 nian and non-Newtonian fluids with different degree of pseudoplasticity
350 $n = [0.45, 1]$.
- 351 • The performance of a generalization method based on the annulus ge-
352 ometry has been tested and found inadequate. Theoretical results for
353 $f \times Re_b^\alpha$ in annulus underestimates the experimental data on average in
354 34% and in 27% in geometries EG1 and EG2 respectively (in laminar
355 region $Re_g < 40$). Furthermore, the representation of the friction factor

356 versus the generalized Reynolds number based on the annulus geome-
357 try is still dependent on the flow behaviour index $f = \Psi(n, Re_{DL,\xi=an})$
358 in the laminar region. Therefore, this generalization is invalid.

- 359 • As suggested by Delplace and Leuliet (1995), an experimental value of
360 ξ in Eq. 8 has been obtained using the experimental data in laminar
361 region ($Re_{DL,an} < 40$). This equation correlates with an error of 17%
362 and 13% in geometries EG1 and EG2 respectively. Furthermore, rep-
363 resentations of f versus $Re_{DL,\xi=exp}$ still shows some dependence on n .
364 This solution is very simple, as it only depends on 1 parameter, but
365 the results can be improved.
- 366 • A more precise and still simple correlation for the generalization method
367 has been proposed. The proposed correlation estimates $f \times Re_b^\alpha$ with
368 an error of 11% and 9% in geometries EG1 and EG2 respectively and
369 the representation of f versus the generalized Reynolds number with
370 this method Re_g shows no appreciable dependence on n .
- 371 • The generalized expressions of the Reynolds number and the viscos-
372 ity obtained in this work are valid for their use in this specific heat
373 exchanger working with any non Newtonian Power Law fluid.
- 374 • The generalized method proposed can be applied to similar heat ex-
375 changer designs with complex non-uniform cross sections.

376 5. Acknowledgements

377 The first author thanks Mr. Martínez and Dr. Solano for their invaluable
378 contribution to the project and their advise. He also thanks the Spanish

379 Government, Ministry of Education for the FPU scholarship referenced as
380 AP2007-03429 which covered the expenses of a 4-year research at *Universidad*
381 *Politécnica de Cartagena*.

- 382 Abdelrahim, K.A., Ramaswamy, H.S., 1995. High temperature/pressure rhe-
383 ology of carboxymethyl cellulose (cmc). *Food Research International* 28,
384 285–290.
- 385 Abu-Jdayil, B., 2003. Modelling the time-dependent rheological behavior of
386 semisolid foodstuffs. *Journal of Food Engineering* 57, 97–102.
- 387 Benchabane, A., Bekkour, K., 2008. Rheological properties of carboxymethyl
388 cellulose (cmc) solutions. *Colloid and Polymer Science* 286, 1173–1180.
- 389 Cancela, M., Alvarez, E., Maceiras, R., 2005. Effects of temperature and
390 concentration on carboxymethylcellulose with sucrose rheology. *Journal of*
391 *Food Engineering* 71, 419–424.
- 392 Chhabra, R., Richardson, J., 2008. Non Newtonian flow and applied rheol-
393 ogy. Engineering applications. Butterworth-Heinemann, 225 Wildwood Av.,
394 Woburn.
- 395 Delplace, F., Leuliet, J., 1995. Generalized reynolds number for the flow
396 of power law fluids in cylindrical ducts of arbitrary cross-section. *The*
397 *Chemical Engineering Journal and the Biochemical Engineering Journal*
398 56, 33 – 37.
- 399 Fernandes, C.S., Dias, R.P., Nabrega, J.M., Maia, J.M., 2007. Laminar flow
400 in chevron-type plate heat exchangers: Cfd analysis of tortuosity, shape
401 factor and friction factor. *Chemical Engineering and Processing: Process*
402 *Intensification* 46, 825 – 833. Selected Papers from the European Process
403 Intensification Conference (EPIC), Copenhagen, Denmark, September 19-
404 20, 2007.

- 405 Fernandes, C.S., Dias, R.P., Nabrega, J.M., Maia, J.M., 2008. Friction factors
406 of power-law fluids in chevron-type plate heat exchangers. *Journal of Food*
407 *Engineering* 89, 441 – 447.
- 408 Fyrippi, I., Owen, I., Escudier, M., 2004. Flowmetering of non-newtonian
409 liquids. *Flow Measurement and Instrumentation* 15, 131–138.
- 410 García, A., Vicente, P., Viedma, A., 2005. Experimental study of heat
411 transfer enhancement with wire coil inserts in laminar-transition-turbulent
412 regimes at different prandtl numbers. *Int. J. Heat Mass Transfer* 48, 4640–
413 4651.
- 414 Ghannam, M.T., Esmail, M.N., 1996. Rheological properties of car-
415 boxymethyl cellulose. *Journal of Applied Polymer Science* 64, 289–301.
- 416 Giri, A.K., Majumder, S.K., 2014. Pressure drop and its reduction of gas-
417 non-newtonian liquid flow in downflow trickle bed reactor (dtbr). *Chemical*
418 *Engineering Research and Design* 92, 34 – 42.
- 419 Gratao, A., Jr., V.S., Telis-Romero, J., 2006. Laminar forced convection
420 to a pseudoplastic fluid food in circular and annular ducts. *International*
421 *Communications in Heat and Mass Transfer* 33, 451 – 457.
- 422 Gratao, A., Jr., V.S., Telis-Romero, J., 2007. Laminar flow of soursop juice
423 through concentric annuli: Friction factors and rheology. *Journal of Food*
424 *Engineering* 78, 1343 – 1354.
- 425 Hartnett, J., Kostic, M., 1985. Heat transfer to a viscoelastic fluid in laminar
426 flow through a rectangular channel. *International Journal of Heat and Mass*
427 *Transfer* 28, 1147–55.

- 428 Hong, S., Bergles, A., 1976. Augmentation of laminar flow heat transfer
429 in tubes by means of twisted-tape inserts. *ASME J. Heat Transfer* 98,
430 251–256.
- 431 Igumentsev, T., Nazmeev, Y., 1978. Intensification of convective heat ex-
432 change by spiral swirlers in the flow of anomalously viscous liquids in
433 pipes. *J. Eng. Phys.* 35, 890–894.
- 434 ISO, 1995. *Guide to the Expression for Uncertainty Measurement*, first ed.
435 International Organization for Standardization, Switzerland.
- 436 Kakaç, S., Shah, R., Aung, W., 1987. *Handbook of single-phase convective*
437 *heat transfer*. A Wiley Interscience publication, Wiley.
- 438 Kozicki, W., Chou, C.H., Tiu, C., 1966. Non-newtonian flow in ducts of
439 arbitrary cross-sectional shape. *Chemical Engineering Science* 21, 665 –
440 679.
- 441 Manglik, R., Bergles, A., Joshi, S., 1988. Augmentation of heat transfer
442 to laminar flow of non-newtonian fluids in uniformly heated tubes with
443 twisted-tape inserts, in: Elsevier (Ed.), *Proceedings of the 1st World Con-*
444 *ference on Experimental Heat Transfer, Fluid Mechanics and Thermody-*
445 *namics*, New York.
- 446 Marner, W., Bergles, A., 1985. Augmentation of highly viscous laminar
447 tubeside heat transfer by means of a twisted-tape insert and an internally
448 finned tube. *ASME HTD* 43, 19–28.
- 449 Martínez, D., García, A., Solano, J., Viedma, A., 2014. Heat transfer en-
450 hancement of laminar and transitional newtonian and non-newtonian flows

451 in tubes with wire coil inserts. *International Journal of Heat and Mass*
452 *Transfer* 76, 540–548.

453 Metzner, A.B., Reed, J.C., 1955. Flow of non-newtonian fluids - correlation
454 of the laminar, transition, and turbulent-flow regions. *Aiche Journal* 1(4),
455 434–440.

456 Nazmeev, Y., 1979. Intensification of convective heat exchange by ribbon
457 swirlers in the flow of anomalously viscous liquids in pipes. *J. Eng. Phys.*
458 37, 910–913.

459 Oliver, D., Shoji, Y., 1992. Heat transfer enhancement in round tubes using
460 different tube inserts: non-newtonian liquids, *trans. IChemE* 70, 558–564.

461 Patil, A., 2000. Laminar flow heat transfer and pressure drop characteristics
462 of power-law fluids inside tubes with varying width twisted tape inserts.
463 *J. Heat Transfer* 122, 143–149.

464 Rene, F., Leuliet, J., Lalande, M., 1991. Heat transfer to newtonian and
465 non- newtonian food fluids in plate heat exchangers: experimental and
466 numerical approaches. *Trans IChemE* 69, 115–126.

467 Solano, J., García, A., Vicente, P., Viedma, A., 2011. Flow field and heat
468 transfer investigation in tubes of heat exchangers with motionless scrapers.
469 *Applied Thermal Engineering* 31, 2013–2024.

470 Webb, R.L., 2005. *Principles of Enhanced Heat Transfer*. Wiley Interscience.

471 Yang, X.H., Zhu, W.L., 2007. Viscosity properties of sodium carboxymethyl-
472 cellulose solutions. *Cellulose* .

473 **List of Figures**

474 1 Analysed geometries. 10

475 2 Experimental set-up. (1) Test fluid tank, (2, 12) gear pumps,
476 (3) frequency converter, (4) immersion resistance, (5) Coriolis
477 flowmeter, (6) temperature sensor and PID controller. (7)
478 pressure transmitter, (8) stainless steel tube with an insert
479 scraper, (9) pressure ports, (10) smooth stainless steel pipe
480 used as viscometer, inlet and outlet immersion RTDs, (11)
481 hydraulic piston (14, 17) centrifugal pumps, (15) three-way
482 valve, (16) coolant liquid tank, (18) cooling machine. 11

483 3 Rheological properties measurement during one of the test. . . 14

484 4 Re_b versus Fanning friction factor for the geometries under
485 study. Only most representative results are shown. 17

486 5 Comparison of $f \times Re_b$ between experimental results and the-
487 theoretical results for annulus. 19

488 6 EG1. $Re_{DL, \xi=an}$ versus Fanning friction factor. 20

489 7 EG2. $Re_{DL, \xi=an}$ versus Fanning friction factor. 21

490 8 Comparison between experimental results and Eq. 12 with the
491 experimental values of ξ (see Table 2) 23

492 9 Generalized Reynolds number with Eq. 12 and the experimen-
493 tal values of ξ (see Table 2). 24

494 10 Comparison between experimental results and experimental
495 correlations. 28

496 11 EG1. Generalized Reynolds number Re_g (Eq. 18) versus Fan-
497 ning friction factor. 29

498	12	EG2. Generalized Reynolds number Re_g (Eq. 18) versus Fan-	
499		ning friction factor.	30